Probing Top-Charm Associated Production at the LHC in the R-parity violating MSSM *

Zhou Hong[b], Ma Wen-Gan[a,b], Jiang Yi[b], Zhang Ren-You[b] and Wan Lang-Hui[b]
[a]CCAST (World Laboratory), P.O.Box 8730, Beijing 100080, China.
[b]Department of Modern Physics, University of Science and Technology
of China (USTC), Hefei, Anhui 230027, China.

Abstract

We present the analytical and numerical investigations of top-charm associated production at the LHC in the framework of the R-parity violating MSSM. The numerical analysis of their production rates is carried out in the mSUGRA scenario with some typical parameter sets. The results show that the cross sections of associated $t\bar{c}(\bar{t}c)$ production via gluon-gluon fusion can reach 5% of that via $d\bar{d}$ annihilation. The total cross section will reach the order of $10 \sim 10^2$ fb and the cross sections are strongly related to the R-parity violating parameters.

PACS number(s): 12.60.Jv, 14.65.-q, 14.65.Ha, 14.65.Dw

*The project supported by National Natural Science Foundation of China

1. INTRODUCTION

There are stringent experimental constraints against the existence of tree-level flavor changing scalar interactions(FCSI's) involving the light quarks. This leads to the suppression of the flavor changing neutral current (FCNC) couplings, an important feature of the standard model (SM), which is explained in terms of the Glashow-Iliopoulos-Maiani(GIM) mechanism [1]. At present, the minimal supersymmetric extension (MSSM)[2] [3] of the standard model (SM) [4][5] is widely considered as the most appealing model. Apart from describing the experimental data as well as the SM does, the supersymmetric (SUSY) theory is able to solve various theoretical problems, such as the fact that the SUSY may provide an elegant way to construct the huge hierarchy between the electroweak symmetry-breaking and the grand unification scales.

FCNC coupling is widely studied for its importance to verify new physics. Searching for FCNC at high energy colliders, particularly e^+e^- colliders was investigated in Ref.[6]. Probing the FCNC vertices $\bar{t}$-c-V(V=γ, Z) in rare decays of top quark and via top-charm associated production were examined in Refs.[7] and [8]-[12], respectively. The effect of the anomalous $\bar{t}-c-g$ coupling on single top quark production via the $q\bar{q}$ process at the Tevatron has been studied in Ref.[13], Here we mention some possible mechanisms which can induce the FCNC couplings:

1. In the Standard Model (SM), the FCNC couplings are strongly suppressed by GIM mechanism. Such interactions can be produced by higher order radiative corrections in the SM, the effect is too small to be observable [8] [14].

2. In models with multiple Higgs doublets such as supersymmetric models and the Two-Higgs-Doublet-Model(THDM) (model III), there would exist possible strong effects of the FCNC [14] [15]. Atwood et al. [9][10] presented the results of a calculation for the process $e^+e^- \to t\bar{c}$(or $\bar{t}c$) in the THDM III. In Ref.[10] [11] [16], the process $\gamma\gamma \to t\bar{c}$(or $\bar{t}c$) in the THDM III and SUSY-QCD, is studied at the Next Linear Collider. The associated product of $t\bar{c}(\bar{t}c)$ via gluon-gluon at hadron colliders was consider by [17]. They all concluded that it would be possible to find associated $t\bar{c}$(or $\bar{t}c$) production events at the NLC, Tevatron and LHC in the THDM (III) and the MSSM. They also showed that the FCNC effects depended on the resonance of Higgs boson. In the MSSM with R-parity conservation, squark mixing can give FCNC couplings. But if we take alignment assumption of S. Dimopoulos [18],it should be very small: mixing between up-type squarks can be even as small as 10^{-3} to 10^{-5} times KM matrix elements.

In the MSSM, if lepton and baryon numbers are conserved, there must be a conservation of a discrete symmetry called R-parity(R_p) conservation[19], which is defined as

$$R_p = (-1)^{3B+L+2S},$$

where B, L and S are the baryon, lepton number and spin of a particle, respectively. In this case, all supersymmetric particles must produced in pair, and the lightest supersymmetric particle must be stable.

However, R_p conservation with both B- and L-number conserved is not necessary to avoid rapid proton decays, instead we just need either B-conservation or L-conservation[20]. In this case the R-parity is not conserved any more and the feature of supersymmetric models are

changed a lot. Due to the lack of experimental tests for R_p conservation, the R_p violation is also equally well motivated in the MSSM. And the models with R_p violation ($\not{R}_p$) are hopeful for us to solve the long standing problems in the particle physics, such as neutrino masses and mixing.

Theoretically R_p-violation models will open some new processes forbidden or highly suppressed in R_p conservation case, but the present low-energy experimental data have put constraints on R_p-violation parameters. Unfortunately, they give only some upper limits on the $\not{R}_p$ parameters, such as B-violating parameters($\lambda^{"}$) and L-violating parameters(λ and $\lambda^{'}$) (The definitions of these $\not{R}_p$ parameters will be presented clearly in sector 2, and their constraints are collected in Ref.[21].). Therefore, trying to find the signal of R_p violation or getting more stringent constraints on the parameters in future experiments is one of the promising tasks.

In the last few years, many efforts were made to find $\not{R}_p$ interactions in experiments. The possible signal of R_p-violation could be the single SUSY particle production or LSP decay, the existence of the difference between the fermion pair production rates in the $\not{R}_p$ MSSM and R_p conservation MSSM, and probing couplings of the flavor changing neutral current(FCNC) et cetera.

In the following years, the hadron colliders, such as Tevatron Run II and the LHC, are the effective machines in searching for new physics. People believe that there will be more experimental events involving top quark collected in the future experiments. It provides an opportunity to study the physics beyond the SM with more precise experimental results.

In this work we will concentrate on the FCNC coupling test and use associated $\bar{t}$c(or t$\bar{c}$) production at LHC to probe R_p violation. Although up to now many constraints from low-energy phenomenology have been given, B-violation parameters involving heavy flavors are still constrained weakly. Such as $\lambda^{"}_{2ij}$ and $\lambda^{"}_{3ij}$, which got strongest constraints from width ratio between Z^0 decaying to leptons and hadrons, can still be order of 1(O(1)). So if these parameters are standing close to present upper limits, R_p-violating effects could be detected on future colliders.

In this paper we present the complete parent process $pp \to t\bar{c}(\bar{t}c)$ including one-loop induced subprocess $gg \to t\bar{c}(\bar{t}c)$ and tree-level subprocess $dd \to t\bar{c}(\bar{t}c)$ in the R-parity violating MSSM theory. The paper is arranged as follows: In Sec.2 we give the analytical calculations of both subprocess and parent process. In Sec.3, the numerical results for subprocess and parent process are illustrated along with discussions. A short summary is presented in Sec.4 . Finally some notations used in this paper, the explicit expressions of the form factors induced by the loop diagrams are collected in Appendix.

2. CALCULATION

The R_p violating MSSM should contain the most general superpotential respecting to the gauge symmetries of the SM, which includes bilinear and trilinear terms and can be expressed as

$$\mathcal{W}_{\not R_p} = \frac{1}{2}\lambda_{[ij]k} L_i . L_j \bar{E}_k + \lambda^{'}_{ijk} L_i . Q_j \bar{D}_k + \frac{1}{2}\lambda^{''}_{i[jk]} \bar{U}_i \bar{D}_j \bar{D}_k + \epsilon_i L_i H_u . \tag{1}$$

where L_i, Q_i are the SU(2) doublet lepton and quark fields, E_i, U_i, D_i are the singlet

superfields. The UDD couplings violate baryon number and the other three sets violate lepton number. In this work we ignored the bilinear term that includes lepton and Higgs superfields for simplicity, because its effects are assumed small in our process[20]. We also forbid explicitly the UDD-type interactions (B-number violation) as a simple way to avoid unacceptable rapid proton decay[22]. Since the couplings in the term of LLE have no contribution to the process $pp \to t\bar{c}(\bar{t}c) + X$ concerned in this paper, we shall not discuss them either.

Expanding the second term of superfield components in Eq.(1) we obtain the interaction Lagrangian that involves quarks and leptons:

$$\mathcal{L}_{LQD} = \lambda'_{ijk}\{\tilde{\nu}_{iL}\bar{d}_{kR}d_{jL} - \tilde{e}_{iL}\bar{d}_{kR}u_{jL} + \tilde{d}_{jL}\bar{d}_{kR}\nu_{iL} - \tilde{u}_{jL}\bar{d}_{kR}e_{iL} + \tilde{d}^{c}_{kR}\nu_{iL}d_{jL} - \tilde{d}^{c}_{kR}e_{iL}u_{jL}\} + h.c. \tag{2}$$

The Feynman diagrams contributing to the tree-level subprocess $d\bar{d} \to t\bar{c}(\bar{t}c)$ in the framework of the $\not{R}_p$-MSSM is depicted in Fig.1(tree-level). In our calculation, we take the 't Hooft-Feynman gauge. The related Feynman rules with $\not{R}_p$ interactions can be read out from Eq.(2). In the following we adopt the notations in Ref.[23] that p_1 and p_2 represent the four-momenta of the incoming particles and k_1 and k_2 represent the four-momenta of the outgoing quarks t and $\bar{c}$ respectively. If we ignore the CP violation, the cross section of $pp \to d\bar{d} \to t\bar{c} + X$ coincides with the process $pp \to d\bar{d} \to \bar{t}c + X$ because of charge conjugation invariance, and the same is also for the loop process $pp \to gg \to t\bar{c} + X$. Therefore, we shall consider only the calculation of the $t\bar{c}$ production in this paper. The corresponding Lorentz-invariant matrix element at the lowest order for the subprocess $d\bar{d} \to t\bar{c}$ is written

as

$$\mathcal{M}(d\bar{d} \to t\bar{c}) = \sum_{\tilde{l}_i^I} \mathcal{M}_{\tilde{l}_i^I}$$

where $\tilde{l}_i^I$ is the partner of lepton l^I, i and I are the mass eigenstate and the generation indeces, respectively. The corresponding differential cross section is obtained by

$$\frac{d\hat{\sigma}}{d\Omega} = \frac{\lambda}{64\pi^2 \hat{s}^2} |\bar{\mathcal{M}}|^2$$

where $\lambda = \sqrt{[\hat{s} - (m_t + m_c)^2]\,[\hat{s} - (m_t - m_c)^2]}$.

For the subprocess of $d\bar{d} \to t\bar{c}$,

$$|\bar{\mathcal{M}}|^2 = \sum_{\tilde{l}_i^I,\ \tilde{l}_j^J} \frac{1}{\hat{t} - m^2_{\tilde{l}_i^I}} \frac{1}{\hat{t} - m^2_{\tilde{l}_j^J}} (k_1 \cdot p_1)(k_2 \cdot p_2) (V^R_{dc\tilde{l}_j^J}{}^* V^R_{dt\tilde{l}_i^I}{}^* V^R_{dc\tilde{l}_i^I} V^R_{dt\tilde{l}_j^J})$$

After integrating over phase space Ω we can get the total section of $d\bar{d} \to t\bar{c}$

$$\begin{aligned}
\hat{\sigma}(d\bar{d} \to t\bar{c}) \;=\; & \frac{1}{64\pi\hat{s}^2} \sum_{\tilde{l}_i^I,\ \tilde{l}_j^J} V^R_{dc\tilde{l}_j^J}{}^* V^R_{dt\tilde{l}_i^I}{}^* V^R_{dc\tilde{l}_i^I} V^R_{dt\tilde{l}_j^J} \times \\
& \left\{ \delta_{\tilde{l}_i^I,\ \tilde{l}_j^J} \left[\lambda \left(1 + \frac{4\beta_{\tilde{l}_i^I}}{\alpha_+ \alpha_-} \right) + (2m^2_{\tilde{l}_i^I} - m_c^2 - m_t^2) \gamma_{\tilde{l}_i^I} \right] \right. \\
+ \;& \left. (1 - \delta_{\tilde{l}_i^I,\ \tilde{l}_j^J}) \left(\lambda + \frac{\beta_{\tilde{l}_i^I} \gamma_{\tilde{l}_i^I}}{m^2_{\tilde{l}_i^I} - m^2_{\tilde{l}_j^J}} - \frac{\beta_{\tilde{l}_j^J} \gamma_{\tilde{l}_j^J}}{m^2_{\tilde{l}_i^I} - m^2_{\tilde{l}_j^J}} \right) \right\}
\end{aligned}$$

where we define the notations as

$$\alpha_\pm = m_c^2 + m_t^2 - 2m^2_{\tilde{l}_i^I} - \hat{s} \pm \lambda,$$

$$\beta_k = (m_c^2 - m_k^2)(m_t^2 - m_k^2),$$

$$\gamma_k = \log \left(\frac{m_c^2 + m_t^2 - 2m_k^2 - \hat{s} + \lambda}{m_c^2 + m_t^2 - 2m_k^2 - \hat{s} - \lambda} \right), \quad (k = \tilde{l}_i^I, \tilde{l}_j^J).$$

In the above equation, the bars over $\mathcal{M}$ mean average over initial spin and color.The δ is the Kronecker delta. The notations for vertices are adopted which are shown in Appendix and $\hat{t} = (p_1 - k_1)^2$.

The subprocess $gg \rightarrow t\bar{c}(\bar{t}c)$ can only be produced through one-loop diagrams at the lowest order. Due to the large gluon luminosity in protons, the contribution of one-loop subprocess $gg \rightarrow t\bar{c}(\bar{t}c)$ to the parent process $pp \rightarrow t\bar{c}(\bar{t}c)$ can be significant. In the calculation of subprocess $gg \rightarrow t\bar{c}(\bar{t}c)$, it is not necessary to consider the renormalization, since the ultraviolet divergence will be cancelled automatically when all the one-loop diagrams in framework of the R_p-violating MSSM are involved. The generic Feynman diagrams of the subprocess are depicted in Fig.1(1-31), where the possible exchange of incoming gluons in Fig.1b are not shown. We denote the reaction of $t\bar{c}$ production via gluon-gluon fusion as:

$$g(p_1, \alpha, \mu)g(p_2, \alpha^{'}, \nu) \longrightarrow t(k_1, \beta)\bar{c}(k_2, \beta^{'}). \tag{3}$$

where p_1 and p_2 denote the four momenta of the incoming gluons, k_1, k_2 denote the four momenta of the outgoing t and $\bar{c}$ respectively, and α,$\alpha^{'}$ are the color indices of the colliding gluons; β, $\beta^{'}$ are the color indices of the produced particles.

The corresponding matrix element of the subprocess $gg \rightarrow t\bar{c}(\bar{t}c)$ can be divided into four parts:

$$\mathcal{M} = \mathcal{M}^{\hat{t}} + \mathcal{M}^{\hat{u}} + \mathcal{M}^{\hat{s}} + \mathcal{M}^{q} \tag{4}$$

$\mathcal{M}^q$ is the amplitude of quartic diagram. The u-channel part can be obtained from the

t-channel part by doing exchanges as shown below:

$$\mathcal{M}^{\hat{u}} = \mathcal{M}^{\hat{t}}(\hat{t} \to \hat{u}, k_1 \leftrightarrow k_2, \mu \leftrightarrow \nu, \alpha \leftrightarrow \alpha^{'}) \tag{5}$$

The corresponding matrix element of the subprocess $gg \to t\bar{c}$ for $\hat{t}$-channel, s-channel and quartic interaction diagrams shown in Fig.1b can be written as:

$$\begin{aligned}
\mathcal{M}^{\hat{t}} &= \epsilon^{\mu}(p_1)\epsilon^{\nu}(p_2)\bar{u}(k_1)\{f_1^{\hat{t}}g_{\mu\nu} + f_2^{\hat{t}}\gamma_\mu\gamma_\nu + f_3^{\hat{t}}k_{1\mu}k_{1\nu} + f_4^{\hat{t}}\gamma_\nu k_{1\mu} + f_5^{\hat{t}}\gamma_\mu k_{1\nu} \\
&+ f_6^{\hat{t}}g_{\mu\nu}\not{p}_1 + f_7^{\hat{t}}\gamma_\mu\gamma_\nu\not{p}_1 + f_8^{\hat{t}}k_{1\mu}k_{1\nu}\not{p}_1 + f_9^{\hat{t}}k_{1\mu}\gamma_\nu\not{p}_1 + f_{10}^{\hat{t}}k_{1\nu}\gamma_\mu\not{p}_1 \\
&+ f_{11}^{\hat{t}}\gamma_5 g_{\mu\nu} + f_{12}^{\hat{t}}\gamma_5\gamma_\mu\gamma_\nu + f_{13}^{\hat{t}}\gamma_5 k_{1\mu}k_{1\nu} + f_{14}^{\hat{t}}k_{1\mu}\gamma_5\gamma_\nu + f_{15}^{\hat{t}}k_{1\nu}\gamma_5\gamma_\mu \\
&+ f_{16}^{\hat{t}}g_{\mu\nu}\gamma_5\not{p}_1 + f_{17}^{\hat{t}}\gamma_5\gamma_\mu\gamma_\nu\not{p}_1 + f_{18}^{\hat{t}}k_{1\mu}k_{1\nu}\gamma_5\not{p}_1 + f_{19}^{\hat{t}}k_{1\mu}\gamma_5\gamma_\nu\not{p}_1 + f_{20}^{\hat{t}}k_{1\nu}\gamma_5\gamma_\mu\not{p}_1\} \\
&\quad v(k_2)T_{\beta c}^{\alpha}T_{c\beta'}^{\alpha'} \\
\mathcal{M}^{\hat{s}} &= \epsilon^{\mu}(p_1)\epsilon^{\nu}(p_2)\bar{u}(k_1)\{f_1^{\hat{s}}g_{\mu\nu} + f_6^{\hat{s}}g_{\mu\nu}\not{p}_1 + f_{11}^{\hat{s}}\gamma_5 g_{\mu\nu} + f_{16}^{\hat{s}}g_{\mu\nu}\gamma_5\not{p}_1\}v(k_2)(T_{\beta c}^{\alpha}T_{c\beta'}^{\alpha'} - T_{\beta c}^{\alpha'}T_{c\beta'}^{\alpha}) \\
\mathcal{M}^{q} &= \epsilon^{\mu}(p_1)\epsilon^{\nu}(p_2)\bar{u}(k_1)\{f_1^{q}g_{\mu\nu} + f_{11}^{q}\gamma_5 g_{\mu\nu}\}v(k_2)(T_{\beta c}^{\alpha}T_{c\beta'}^{\alpha'} + T_{\beta c}^{\alpha'}T_{c\beta'}^{\alpha})
\end{aligned}$$

where T_{ij}^{a} are the 3×3 SU(3) color matrices introduce by Gell-Mann [24]. We divide each form factor $f_i^{\hat{t}}$ into follows

$$f_i^{\hat{t}} = f_i^{b,\hat{t}} + f_i^{v,\hat{t}} + f_i^{s,\hat{t}} \quad (i = 1 - 20)$$

The explicit expressions of form factors are collected in Appendix. The cross section for this subprocess at one loop order via unpolarized gluon collisions can be got by using the following equation,

$$\hat{\sigma}(\hat{s}, gg \to t\bar{c}) = \frac{1}{16\pi\hat{s}^2}\int_{\hat{t}^-}^{\hat{t}^+} d\hat{t}\ \bar{\sum}|\mathcal{M}|^2. \tag{6}$$

In above equation, $\hat{t}$ is the momentum transfer squared from one of the incoming gluons to the quark in the final state, and

$$\hat{t}^{\pm} = \frac{1}{2}\left[(m_t^2 + m_c^2 - \hat{s}) \pm \sqrt{(m_t^2 + m_c^2 - \hat{s})^2 - 4m_t^2 m_c^2}\right].$$

The bar over the sum means average over initial spin and color. With the results from Eq.(6), we can easily obtain the total cross section at pp collider by folding the cross section of subprocess $\hat{\sigma}(gg \to t\bar{c})$ with the gluon luminosity.

$$\sigma(s, pp \to gg \to t\bar{c} + X) = \int_{(m_t+m_c)^2/s}^{1} d\tau \frac{d\mathcal{L}_{gg}}{d\tau} \hat{\sigma}(gg \to t\bar{c} \quad at \quad \hat{s} = \tau s), \tag{7}$$

where $\sqrt{s}$ and $\sqrt{\hat{s}}$ are the pp and gg c.m.s. energies respectively and $d\mathcal{L}_{gg}/d\tau$ is the distribution function of gluon luminosity, which is defined as

$$\frac{d\mathcal{L}_{gg}}{d\tau} = \int_{\tau}^{1} \frac{dx_1}{x_1}\left[f_g(x_1, Q^2) f_g(\frac{\tau}{x_1}, Q^2)\right]. \tag{8}$$

here $\tau = x_1\ x_2$, the definition of x_1 and x_2 are from [25], and in our calculation we adopt the MRS set G parton distribution function [26]. The factorization scale Q was chosen as the average of the final particles masses $\frac{1}{2}(m_t + m_c)$. The total cross section contributed by the subprocess $d\bar{d} \to t\bar{c}(\bar{t}c)$ can be obtained by the same way claimed above. The total cross section of $pp \to t\bar{c} + \bar{t}c + X$ is obtained by the cross section of $pp \to t\bar{c} + X$ multiplied by factor 2.

3. Numerical results and discussions

In the following numerical evaluation, we present the numerical results of the cross sections for the $t\bar{c}(\bar{t}c)$ production in the subprocesses and parent process. The parameters originating from the SM are chosen as: quark and lepton mass parameters are obtained from Ref.[27]. We take a simple one-loop formula for the running strong coupling constant α_s. We set $\alpha_s(m_Z) = 0.117$ and $n_f = 5$.

The R-parity violating parameters involvd in the evaluation are set to be $\lambda'_{1ij} = \lambda'_{2ij} = \lambda'_{3ij} = 0.15$ unless otherwise stated explicitly. As we know that the effects of the R-parity violating couplings on the renormalization group equations(RGE's) are the crucial ingredient of mSUGRA-type models, and the complete 2-loop RGE's of the superpotential parameters for the supersymmetric standard model including the full set of R-parity violating couplings are given in Ref.[21]. But in our numerical presentation to get the low energy scenario from the mSUGRA [28], we ignored those effects in the RGE's for simplicity and use the program ISAJET 7.44. In this program the RGE's [29] are run from the weak scale m_Z up to the GUT scale, taking all thresholds into account and using two loop RGE's only for the gauge couplings and the one-loop RGE's for the other supersymmetric parameters. The GUT scale boundary conditions are imposed and the RGE's are run back to m_Z, again taking threshold into account.The R-parity violating parameters chosen above satisfy the constraints given by [20].

Figure 2 shows the cross sections as a function of $\sqrt{\hat{s}}$, and the upper curve corresponds to the subprocess $d\bar{d} \to t\bar{c}$ and the lower curve corresponds to the subprocess $gg \to t\bar{c}$. The input parameters are chosen as $m_0 = 180\ GeV, m_{\frac{1}{2}} = 150\ GeV, A_0 = 200\ GeV, \tan\beta =$

$4, sign(\mu) = +$. With above parameters, we get $m_{\tilde{b}_1} = 353\ GeV, m_{\tilde{b}_2} = 375\ GeV, m_{\tilde{d}_1} = m_{\tilde{s}_1} = 375\ GeV, m_{\tilde{d}_2} = m_{\tilde{s}_2} = 390\ GeV$ in the framework of the mSUGRA. Due to the threshold effects, we can see sharp rising peaks around $\sqrt{\hat{s}} \sim 180\ GeV$ on the two curves in Figure 2, where the threshold condition $\sqrt{\hat{s}} \sim m_t + m_c$ is satisfied. For the subprocess $gg \to t\bar{c}$, when $\sqrt{\hat{s}}$ approaches the value of $2m_{\tilde{d}}$, the cross section will be enhanced by the resonance effects. The small peak on the curve of subprocess $gg \to t\bar{c}$, where $\sqrt{\hat{s}} \sim 2m_{\tilde{d}} \simeq 780\ GeV$, comes from the resonant effect of the quartic diagrams.

The integrated cross sections versus $\tan\beta$ are depicted in Figure 3 and versus m_0 in Figure 4, respectively. We calculate the $t\bar{c} + \bar{t}c$ production cross sections at the LHC with the energies of $\sqrt{s}$ being 14 TeV. In Figure 3 the input parameters are chosen as $m_0 = 150\ GeV, m_{\frac{1}{2}} = 150\ GeV, A_0 = 200\ GeV, sign(\mu) = +$, and in Figure 4 as $m_{\frac{1}{2}} = 150\ GeV, A_0 = 200\ GeV, \tan\beta = 4, sign(\mu) = +$. In both figures, the dotted lines are the curves contributed by $d\bar{d} \to t\bar{c} + \bar{t}c$, the dashed lines are the curves contributed by $gg \to t\bar{c} + \bar{t}c$ and the solid lines are the curves of total cross sections which are the sum of the above two subprocesses. Usually it is shown that the cross section contribution to parent process at hadron collider from subprocess $gg \to t\bar{c} + \bar{t}c$ can be about 5% of that from subprocess $d\bar{d} \to t\bar{c} + \bar{t}c$. So the production mechanism of subprocess $gg \to t\bar{c} + \bar{t}c$ should be considered in detecting the $\not{R}_p$ signals in this parameter space.

In Figure 3 $\tan\beta$ varies from 2 to 30. The total cross section decreases first and at the position of $\tan\beta \simeq 5$ it arrives the nadir, then it increase slightly. The cross section via $pp \to d\bar{d} \to t\bar{c}$ has the same feature, but the curve for the cross section via $pp \to gg \to t\bar{c}$

has little different. In the framework of the mSUGRA, when m_0 varies from 180 GeV to 300 GeV, $m_{\tilde{d}}$ ranges from 370 GeV to 440 GeV. So we can see in Figure 4 that the cross section decreases rapidly with the increment of m_0.

Finally, we will focus on the relationship between the $\bar{t}c + t\bar{c}$ production cross section at the LHC and the R_p-violation parameters $\lambda^{'}_{ijk}$. The sensitivity of the cross section of parents process $pp \to d\bar{d}(gg) \to \bar{t}c + t\bar{c}$ to $\lambda^{'}_{331} * \lambda^{'}_{321}$ with other $\lambda^{'}_{ijk}$'s being taken as 0.15, are shown in Figure 5 in the mSUGRA scenario, where the input parameters m_0, $m_{\frac{1}{2}}$, A_0, $\tan\beta$, $sign(\mu)$ are taken as the same as the corresponding ones in Figure 2. The dotted line is the curve contributed by subprocess $d\bar{d} \to t\bar{c} + \bar{t}c$, the dashed line is the curve contributed by $gg \to t\bar{c} + \bar{t}c$. The cross sections of the both subprocesses are all the functions of $((\lambda^{'}_{331} * \lambda^{'}_{321}))^2$. Therefore, the dependence of the production cross section of $t\bar{c} + \bar{t}c$ on the values of $\lambda^{'}_{ijk}$ is very strong. In the allowable parameter space of $\lambda^{'}_{ijk}$ [21], the cross sections will cover a great range. Similar with the case of the L-number violating case, in the B-number violating case, the R_p-violation parameters $\lambda^{"}_{ijk}$ could play significant role also in the top-charm associated production at the LHC, but we will not discuss it in details in this paper.

4. Summary

In this paper, we have studied the production of top-charm associated production with explicit R_p-violation at the LHC. The production rates via $d - \bar{d}$ annihilation and gluon-gluon fusion at the LHC are presented analytically and numerically in the mSUGRA scenario

with some typical parameter sets. The results show that the cross section of the top-charm associated production at the LHC via gluon-gluon collisions can reach about several femto barn with our chosen parameters, and is usually about 5% of that via quark-antiquark annihilation subprocess. It means that the contribution from $gg \to t\bar{c}(\bar{t}c)$ subprocess can be competitive with that via $d\bar{d} \to t\bar{c}(\bar{t}c)$ subprocess at the LHC and can be considered as an important part of the NLO QCD correction to the $pp \to t\bar{c}(\bar{t}c) + X$ subprocess. Therefore, in detecting the top-charm associated production at the LHC in searching for the signals of SUSY and R_p violation, we should consider not only the associated $t\bar{c}(\bar{t}c)$ production via quark-antiquark annihilation, but also that via the gluon-gluon fusion. By taking an annual luminosity at the LHC being 100 fb^{-1}, one may accumulate 10^3 $t\bar{c}(\bar{t}c)$ production events per year.

Appendix

The relevant Feynman rules concerned in this work are list below:

$$\begin{aligned} \bar{D} - U - \tilde{L}_i \quad &: \quad V^R_{d^K u^J \tilde{l_i}^I}\ P_R \\ \bar{U} - \bar{L} - \tilde{D}_i \quad &: \quad V^L_{\tilde{d_i}^K l^I u^J}\ P_L\ C \end{aligned}$$

where C is the charge conjugation operator, $P_{L,R} = \frac{1}{2}(1 \mp \gamma_5)$. The vertices can be read out from Eq.(2):

$$\begin{aligned} V^R_{d^K u^J \tilde{l_1}^I} &= i\lambda^{'}_{IJK} \cos\theta_{\tilde{L}} \qquad V^R_{d^K u^J \tilde{l_2}^I} = i\lambda^{'}_{IJK} \sin\theta_{\tilde{L}} \\ V^L_{\tilde{d_1}^K l^I u^J} &= -i\lambda^{'}_{IJK} \sin\theta_{\tilde{D}} \qquad V^L_{\tilde{d_2}^K l^I u^J} = i\lambda^{'}_{IJK} \cos\theta_{\tilde{D}} \end{aligned}$$

We adopt the same definitions of one-loop A, B, C and D integral functions as in Ref.[30] and the references therein. All the vector and tensor integrals can be deduced in the forms of scalar integrals [31]. The dimension $D = 4 - \epsilon$. The integral functions are defined as

$$A_0(m) = -\frac{(2\pi\mu)^{4-D}}{i\pi^2}\int d^D q \frac{1}{[q^2 - m^2]},$$

$$\{B_1; B_\mu; B_{\mu\nu}\}(p, m_1, m_2) = \frac{(2\pi\mu)^{4-D}}{i\pi^2}\int d^D q \frac{\{1; q_\mu; q_{\mu\nu}\}}{[q^2 - m_1^2][(q+p)^2 - m_2^2]},$$

$$\{C_0; C_\mu; C_{\mu\nu}; C_{\mu\nu\rho}\}(p_1, p_2, m_1, m_2, m_3) = -\frac{(2\pi\mu)^{4-D}}{i\pi^2}$$

$$\times \int d^D q \frac{\{1; q_\mu; q_{\mu\nu}; q_{\mu\nu\rho}\}}{[q^2 - m_1^2][(q+p_1)^2 - m_2^2][(q+p_1+p_2)^2 - m_3^2]},$$

$$\{D_0; D_\mu; D_{\mu\nu}; D_{\mu\nu\rho}; D_{\mu\nu\rho\alpha}\}(p_1, p_2, p_3, m_1, m_2, m_3, m_4) = \frac{(2\pi\mu)^{4-D}}{i\pi^2}$$

$$\times \int d^D q \{1; q_\mu; q_{\mu\nu}; q_{\mu\nu\rho}; q_{\mu\nu\rho\alpha}\}$$

$$\times \{[q^2 - m_1^2][(q+p_1)^2 - m_2^2][(q+p_1+p_2)^2 - m_3^2][(q+p_1+p_2+p_3)^2 - m_4^2]\}^{-1}.$$

In this appendix, we use the notations defined below for abbreviation:

$$\begin{aligned}
B_0^{(1)}, B_1^{(1)} &= B_0, B_1\left[-k_1, m_{\tilde{d}_i^I}, m_{l^J}\right] \\
B_0^{(2)}, B_1^{(2)} &= B_0, B_1\left[-k_1, m_{\tilde{l}_i^J}, m_{d^I}\right] \\
B_0^{(3)}, B_1^{(3)} &= B_0, B_1\left[-k_2, m_{\tilde{d}_i^I}, m_{l^J}\right] \\
B_0^{(4)}, B_1^{(4)} &= B_0, B_1\left[-k_2, m_{\tilde{l}_i^J}, m_{d^I}\right] \\
B_0^{(5)}, B_1^{(5)} &= B_0, B_1\left[k_1 - p_1, m_{\tilde{d}_i^I}, m_{l^J}\right] \\
B_0^{(6)}, B_1^{(6)} &= B_0, B_1\left[k_1 - p_1, m_{\tilde{l}_i^J}, m_{d^I}\right]
\end{aligned}$$

$$
\begin{aligned}
B_0^{(7)} &= B_0\left[p_1, m_{d^I}, m_{d^I}\right] \\
C_0^{(1)}, C_{ij}^{(1)} &= C_0, C_{ij}\left[-k_1, p_1, l^J, m_{\tilde{d}_i^I}, m_{\tilde{d}_i^I}\right] \\
C_0^{(2)}, C_{ij}^{(2)} &= C_0, C_{ij}\left[-k_1, p_1, m_{\tilde{l}_i^J}, m_{d^I}, m_{d^I}\right] \\
C_0^{(3)}, C_{ij}^{(3)} &= C_0, C_{ij}\left[k_1, -p_1-p_2, m_{l^J}, m_{\tilde{d}_i^I}, m_{\tilde{d}_i^I}\right] \\
C_0^{(4)}, C_{ij}^{(4)} &= C_0, C_{ij}\left[k_1, -p_1-p_2, m_{\tilde{l}_i^J}, m_{d^I}, m_{d^I}\right] \\
C_{ij}^{(5)} &= C_0, C_{ij}\left[-p_2, k_1-p_1, m_{\tilde{d}_i^I}, m_{\tilde{d}_i^I}, m_{l^J}\right] \\
C_0^{(6)}, C_{ij}^{(6)} &= C_0, C_{ij}\left[-p_2, k_1-p_1, m_{d^I}, m_{d^I}, m_{\tilde{l}_i^J}\right] \\
C_0^{(7)}, C_{ij}^{(7)} &= C_0, C_{ij}\left[k_2, k_1, m_{\tilde{d}_i^I}, m_{l^J}, m_{\tilde{d}_i^I}\right] \\
D_0^{(1)}, D_{ij}^{(1)}, D_{ijk}^{(1)} &= D_0, D_{ij}, D_{ijk}\left[k_1, -p_1, -p_2, m_{l^J}, m_{\tilde{d}_i^I}, m_{\tilde{d}_i^I}, m_{\tilde{d}_i^I}\right] \\
D_0^{(2)}, D_{ij}^{(2)}, D_{ijk}^{(2)} &= D_0, D_{ij}, D_{ijk}\left[k_1, -p_1, -p_2, m_{\tilde{l}_i^J}, m_{d^I}, m_{d^I}, m_{d^I}\right] \\
F^V &= -V_{\tilde{d}_i^I l^J c}^{L*} V_{\tilde{d}_i^I l^J t}^{L} \\
E^V &= V_{d^I c \tilde{l}_i^J}^{R} V_{d^I t \tilde{l}_i^J}^{R*} \\
\mathcal{P}_1 &= \frac{1}{\hat{s}} \\
\mathcal{P}_2 = \frac{1}{k_1^2 - m_c^2} \qquad & \mathcal{P}_3 = \frac{1}{k_2^2 - m_t^2} \\
\mathcal{P}_4 = \frac{1}{\hat{t} - m_c^2} \qquad & \mathcal{P}_5 = \frac{1}{\hat{t} - m_t^2}
\end{aligned}
$$

where the upper and lower indexes I, J and K appearing in above variables denote the generation numbers ($I, J, K = 1, 2, 3$), and lower indexes i appearing in the supersymmetric quarks ($\tilde{u}_i$), ($\tilde{d}_i$) and lepton ($\tilde{l}_i$) can be 1 and 2.

We use the denotation $\mathcal{T}$ in below to represent the replacement of $(E^V \to F^V, m_{\tilde{l}_i^J} \to m_{\tilde{d}_i^I}, m_{d^I} \to m_{l^J})$ for the terms appearing before $\mathcal{T}$ in the same level parentheses. We listed the expressions of f_1 to f_{10} only and the others can obtained the transformation, $f_{i+10} = -f_i(m_t \to -m_t), i = 1 \sim 10$. The factors f_i we don't mention below, are zero.

The form factors of the amplitude part from t-channel box diagrams are written as

$$
\begin{aligned}
f_1^{b,\hat{t}} &= \frac{ig_s^2}{8\pi^2}\Big\{E^V\Big[-D_{313}^{(2)}m_c + (-D_{311}^{(2)} + D_{313}^{(2)})m_t\Big] + \mathcal{T} - E^V D_{27}^{(2)} m_t\Big\} \\
f_2^{b,\hat{t}} &= \frac{ig_s^2}{32\pi^2}E^V\Big[(2D_{27}^{(2)} + 6D_{313}^{(2)})m_c + (-D_{13}^{(2)} - D_{25}^{(2)} - D_{37}^{(2)} - D_{23}^{(2)})m_c^3 \\
&+ (4D_{27}^{(2)} + 6D_{311}^{(2)} - 6D_{313}^{(2)})m_t + (D_{23}^{(2)} - D_{25}^{(2)} - D_{35}^{(2)} + D_{37}^{(2)})m_c^2 m_t \\
&+ (-D_0^{(2)} - 2D_{11}^{(2)} + D_{12}^{(2)} - D_{21}^{(2)} + D_{24}^{(2)} - D_{25}^{(2)} + D_{310}^{(2)} - D_{35}^{(2)} + D_{26}^{(2)})m_c m_t^2 \\
&+ (-D_{21}^{(2)} + D_{24}^{(2)} + D_{25}^{(2)} - D_{26}^{(2)} - D_{310}^{(2)} - D_{31}^{(2)} + D_{34}^{(2)} + D_{35}^{(2)})m_t^3 \\
&+ (D_{25}^{(2)} + D_{37}^{(2)} - D_{26}^{(2)} - D_{39}^{(2)})m_c\hat{s} + (D_{35}^{(2)} - D_{37}^{(2)} - D_{310}^{(2)} + D_{39}^{(2)})m_t\hat{s} \\
&+ (-D_{12}^{(2)} - D_{24}^{(2)} - D_{310}^{(2)} + D_{37}^{(2)} + D_{23}^{(2)} - D_{26}^{(2)})m_c\hat{t} + (D_0^{(2)} + D_{13}^{(2)})m_c m_{d^I}^2 + (D_{11}^{(2)} - D_{13}^{(2)})m_t m_{d^I}^2 \\
&+ (-D_{11}^{(2)} + D_{13}^{(2)} - D_{21}^{(2)} - D_{23}^{(2)} - D_{24}^{(2)} + 2D_{25}^{(2)} + D_{26}^{(2)} + D_{310}^{(2)} - D_{34}^{(2)} + D_{35}^{(2)} - D_{37}^{(2)})m_t\hat{t}\Big] \\
f_3^{b,\hat{t}} &= \frac{ig_s^2}{8\pi^2}\Big\{E^V\Big[(D_{13}^{(2)} + 2D_{25}^{(2)} + D_{35}^{(2)})m_c + (D_{11}^{(2)} \\
&- D_{13}^{(2)} + 2D_{21}^{(2)} - 2D_{25}^{(2)} + D_{31}^{(2)} - D_{35}^{(2)})m_t\Big] + \mathcal{T}\Big\} \\
f_4^{b,\hat{t}} &= \frac{ig_s^2}{16\pi^2}\Big\{E^V\Big[-2D_{311}^{(2)} + 6D_{313}^{(2)} + (-D_{13}^{(2)} - D_{25}^{(2)} - D_{37}^{(2)} - D_{23}^{(2)})m_c^2 \\
&+ (D_0^{(2)} + 2D_{11}^{(2)} + D_{21}^{(2)})m_c m_t + (-D_{25}^{(2)} + D_{310}^{(2)} - D_{35}^{(2)} + D_{26}^{(2)})m_t^2 + (D_{25}^{(2)} + D_{37}^{(2)} - D_{26}^{(2)} \\
&- D_{39}^{(2)})\hat{s} + (-D_{310}^{(2)} + D_{37}^{(2)} - D_{26}^{(2)} + D_{23}^{(2)})\hat{t} + (D_0^{(2)} + D_{13}^{(2)})m_{d^I}^2\Big] + 2F^V(-D_{27}^{(1)} - D_{311}^{(1)})\Big\} \\
f_5^{b,\hat{t}} &= \frac{ig_s^2}{16\pi^2}\Big\{2E^V(D_{27}^{(2)} + D_{311}^{(2)}) - \mathcal{T} + E^V\Big[2D_{311}^{(2)} - 6D_{313}^{(2)}
\end{aligned}
$$

$$
\begin{aligned}
&+ \quad (D^{(2)}_{23} - D^{(2)}_{25} - D^{(2)}_{35} + D^{(2)}_{37})m_c^2 + (-D^{(2)}_{11} + D^{(2)}_{13} - 2D^{(2)}_{21} + D^{(2)}_{24} + 2D^{(2)}_{25} - D^{(2)}_{26} \\
&- \quad D^{(2)}_{310} - D^{(2)}_{31} + D^{(2)}_{34} + D^{(2)}_{35})m_t^{(2)} + (-D^{(2)}_{310} + D^{(2)}_{39} + D^{(2)}_{35} - D^{(2)}_{37})\hat{s} \\
&+ \quad (D^{(2)}_{35} - D^{(2)}_{37} - D^{(2)}_{23} - D^{(2)}_{24} + D^{(2)}_{25} + D^{(2)}_{26} + D^{(2)}_{310} - D^{(2)}_{34})\hat{t} + (D^{(2)}_{11} - D^{(2)}_{13})m^2_{d^I}\Big]\Big\} \\
f_6^{b,\hat{t}} &= \frac{ig_s^2}{8\pi^2}\Big[E^V(D^{(2)}_{312} - D^{(2)}_{313}) + \mathcal{T} + E^V D^{(2)}_{27}\Big] \\
f_7^{b,\hat{t}} &= \frac{ig_s^2}{32\pi^2}E^V\Big[-2D^{(2)}_{27} - 6D^{(2)}_{312} + 6D^{(2)}_{313} + (D^{(2)}_0 + D^{(2)}_{11})m_c m_t \\
&+ \quad (-D^{(2)}_{13} - D^{(2)}_{25} + D^{(2)}_{310} - D^{(2)}_{37} - D^{(2)}_{23} + D^{(2)}_{26})m_c^2 \\
&+ \quad (-D^{(2)}_{11} + D^{(2)}_{12} - D^{(2)}_{21} - D^{(2)}_{22} + 2D^{(2)}_{24} - D^{(2)}_{25} + D^{(2)}_{310} + D^{(2)}_{34} - D^{(2)}_{35} - D^{(2)}_{36} + D^{(2)}_{26})m_t^2 \\
&+ \quad (+D^{(2)}_{25} - D^{(2)}_{310} + D^{(2)}_{37} - D^{(2)}_{26} + D^{(2)}_{38} - D^{(2)}_{39})\hat{s} + (D^{(2)}_{22} - 2D^{(2)}_{26} - 2D^{(2)}_{310} \\
&+ \quad D^{(2)}_{36} + D^{(2)}_{37} + D^{(2)}_{23})\hat{t} + (D^{(2)}_0 - D^{(2)}_{12} + D^{(2)}_{13})m^2_{d^I}\Big] \\
f_8^{b,\hat{t}} &= \frac{ig_s^2}{8\pi^2}\Big[E^V(-D^{(2)}_{24} + D^{(2)}_{25} - D^{(2)}_{34} + D^{(2)}_{35}) + \mathcal{T} + F^V(-D^{(1)}_{12} + D^{(1)}_{13} - D^{(1)}_{24} + D^{(1)}_{25})\Big] \\
f_9^{b,\hat{t}} &= \frac{ig_s^2}{16\pi^2}E^V\Big[D^{(2)}_{12} + D^{(2)}_{24})m_c + (D^{(2)}_{11} - D^{(2)}_{12} + D^{(2)}_{21} - D^{(2)}_{24})m_t\Big] \\
f_{10}^{b,\hat{t}} &= \frac{ig_s^2}{16\pi^2}E^V\Big[(-D^{(2)}_{13} - D^{(2)}_{25})m_c + (-D^{(2)}_{11} + D^{(2)}_{13} - D^{(2)}_{21} + D^{(2)}_{25})m_t\Big]
\end{aligned}
$$

The form factors of the amplitude part from t-channel vertex diagrams are written as

$$
\begin{aligned}
f_2^{v,\hat{t}} &= \frac{ig_s^2}{64\pi^2}\Big\{2\mathcal{P}_5(\hat{t} - m_t^2)C^{(6)}_{12}E^V m_c + \mathcal{P}_4\Big[E^V((m_c - m_t)(1 - 4C^{(2)}_{24} - 2C^{(2)}_0 m^{(2)}_{d^I}) \\
&+ \quad 2(C^{(2)}_{11} + C^{(2)}_{21})m_t^2 + 2(C^{(2)}_{12} + C^{(2)}_{23})(\hat{t} - m_t^2)) - 2(C^{(2)}_{11} + C^{(2)}_0)m_t(\hat{t} - m_t m_c)) \\
&+ \quad 4C^{(1)}_{24}F^V(m_c - m_t)\Big]\Big\} \\
f_3^{v,\hat{t}} &= \frac{ig_s^2}{8\pi^2}\mathcal{P}_5\Big\{E^V\Big[(-C^{(6)}_{12} - C^{(6)}_{23})m_c + (C^{(6)}_{23} - C^{(6)}_{22})m_t\Big] + \mathcal{T}\Big]
\end{aligned}
$$

$$
\begin{aligned}
f_4^{v,\hat{t}} &= \frac{ig_s^2}{32\pi^2}\Big\{\mathcal{P}_5\Big[E^V(1-4C_{24}^{(6)}+2(C_{12}^{(6)}+C_{23}^{(6)})m_c^2+2(C_{22}^{(6)}-C_{23}^{(6)})\hat{t}-2C_0^{(6)}m_{d^I}^2+2C_{12}^{(6)}m_cm_t) \\
&+ 4C_{24}^{(5)}F^V\Big]+2\mathcal{P}_4\Big[E^V(2C_{24}^{(2)}+(C_{23}^{(2)}-C_{21}^{(2)})m_t^2-C_{23}^{(2)}\hat{t}-(C_{11}^{(2)}+C_{21}^{(2)})m_tm_c)+\mathcal{T} \\
&+ E^V\Big[-B_0^{(7)}-C_0^{(2)}m_{d^I}^2+C_0^{(2)}m_{\tilde{l}_i^J}^2-(C_0^{(2)}+C_{11}^{(2)})m_tm_c\Big]+F^V\Big[(-C_{11}^{(1)}+C_{12}^{(1)})m_t^2-C_{12}^{(1)}\hat{t}\Big]\Big]\Big\} \\
f_5^{v,\hat{t}} &= \frac{ig_s^2}{16\pi^2}\mathcal{P}_5\Big[(C_{23}^{(6)}-C_{22}^{(6)})E^V(\hat{t}-m_t^2)+\mathcal{T}\Big] \\
f_7^{v,\hat{t}} &= \frac{ig_s^2}{64\pi^2}\Big\{\mathcal{P}_5\Big[E^V(1-4C_{24}^{(6)}+2(C_{12}^{(6)}+C_{23}^{(6)})m_c^2+2(C_{22}^{(6)}-C_{23}^{(6)})\hat{t}-2C_0^{(6)}m_{d^I}^2+2C_{12}^{(6)}m_cm_t) \\
&+ 4C_{24}^{(5)}F^V\Big]+\mathcal{P}_4\Big[E^V(1-4C_{24}^{(2)}+2(C_{11}^{(2)}-C_{12}^{(2)}+C_{21}^{(2)}-C_{23}^{(2)})m_t^2 \\
&+ 2(C_{12}^{(2)}+C_{23}^{(2)})\hat{t}-2C_0^{(2)}m_{d^I}^2-2(C_0^{(2)}+C_{11}^{(2)})m_tm_c)+4C_{24}^{(1)}F^V\Big]\Big\} \\
f_9^{v,\hat{t}} &= \frac{ig_s^2}{16\pi^2}\mathcal{P}_4\Big\{E^V\Big[(-C_{11}^{(2)}+C_{12}^{(2)}-C_{21}^{(2)}+C_{23}^{(2)})m_t+(-C_{12}^{(2)}-C_{23}^{(2)})m_c\Big]+\mathcal{T}\Big\} \\
f_{10}^{v,\hat{t}} &= \frac{ig_s^2}{16\pi^2}\mathcal{P}_5\Big\{E^V\Big[(C_{12}^{(6)}+C_{23}^{(6)})m_c+(-C_{23}^{(6)}+C_{22}^{(6)})m_t\Big]+\mathcal{T}\Big\}
\end{aligned}
$$

The form factors of the amplitude part from t-channel self-energy diagrams are written as

$$
\begin{aligned}
f_2^{s,\hat{t}} &= \frac{ig_s^2}{32\pi^2}E^V\Big[-\mathcal{P}_2\mathcal{P}_4(B_0^{(2)}+B_1^{(2)})(m_t^2-m_c^2)m_t+\mathcal{P}_4\mathcal{P}_5(B_0^{(6)}+B_1^{(6)})(\hat{t}-m_t^2)m_c\Big]-\mathcal{T} \\
f_4^{s,\hat{t}} &= \frac{ig_s^2}{16\pi^2}E^V\Big[\mathcal{P}_2\mathcal{P}_4(B_0^{(2)}+B_1^{(2)})(m_t+m_c)m_t+\mathcal{P}_3\mathcal{P}_5(B_0^{(4)}+B_1^{(4)})(m_t+m_c)m_c \\
&+ \mathcal{P}_4\mathcal{P}_5(B_0^{(6)}+B_1^{(6)})(\hat{t}+m_tm_c)\Big]-\mathcal{T} \\
f_7^{s,\hat{t}} &= \frac{ig_s^2}{32\pi^2}E^V\Big[\mathcal{P}_2\mathcal{P}_4(B_0^{(2)}+B_1^{(2)})(m_t+m_c)m_t+\mathcal{P}_3\mathcal{P}_5(B_0^{(4)}+B_1^{(4)})(m_t+m_c)m_c \\
&+ \mathcal{P}_4\mathcal{P}_5(B_0^{(6)}+B_1^{(6)})(\hat{t}+m_tm_c)\Big]-\mathcal{T}
\end{aligned}
$$

The form factors of the amplitude part from s-channel diagrams are written as

$$
\begin{aligned}
f_1^{\hat{s}} &= \frac{ig_s^2}{64\pi^2}\mathcal{P}_1\Big\{E^V\Big[(-2\mathcal{P}_2(B_0^{(2)}+B_1^{(2)})(m_t^2-m_c^2)m_t - 2\mathcal{P}_3(B_0^{(4)}+B_1^{(4)})(m_t^2-m_c^2)m_c - \mathcal{T}) \\
&+ (m_c-m_t)(1-4C_{24}^{(4)}-2C_0^{(4)}m_{d^I}^2) + 2(C_0^{(4)}+2C_{11}^{(4)}-C_{12}^{(4)}+C_{21}^{(4)}-2C_{23}^{(4)}+C_{22}^{(4)})m_c m_t^2 \\
&+ 2(C_{12}^{(4)}+C_{22}^{(4)})m_c^3 + 2(C_{12}^{(4)}+2C_{23}^{(4)}-C_{22}^{(4)})m_c\hat{t} + 2(-C_{12}^{(4)}-{}_{22}^{(4)})m_c\hat{u} \\
&+ 2(-C_0^{(4)}-C_{11}^{(4)}-C_{12}^{(4)}-C_{22}^{(4)})m_c^2 m_t + 2(-C_{11}^{(4)}+C_{12}^{(4)}-C_{21}^{(4)}+2C_{23}^{(4)}-C_{22}^{(4)})m_t^3 \\
&+ 2(C_{11}^{(4)}-C_{12}^{(4)}+C_{21}^{(4)}-2C_{23}^{(4)}+C_{22}^{(4)})m_t\hat{t} + 2(-C_{11}^{(4)}+C_{12}^{(4)}-C_{21}^{(4)}+C_{22}^{(4)})m_t\hat{u}\Big] \\
&+ 2F^V\Big[2C_{24}^{(3)}(m_c-m_t) + (C_{12}^{(3)}+C_{23}^{(3)})(m_c-m_t)(\hat{t}-\hat{u}) + (C_{11}^{(3)}+C_{21}^{(3)})m_t(\hat{t}-\hat{u})\Big]\Big\} \\
f_6^{\hat{s}} &= \frac{ig_s^2}{32\pi^2}\mathcal{P}_1\Big\{E^V\Big[(2\mathcal{P}_2(B_0^{(2)}+B_1^{(2)})(m_t+m_c)m_t + 2\mathcal{P}_3(m_t+m_c)(B_0^{(4)}+B_1^{(4)})m_c - \mathcal{T}) \\
&+ 1-4C_{24}^{(4)} + 2(C_{12}^{(4)}+C_{23}^{(4)})m_c^2 - 2(C_0^{(4)}+C_{11}^{(4)})m_c m_t + 2(C_{11}^{(4)}+C_{21}^{(4)}-C_{12}^{(4)}-C_{23}^{(4)})m_t^2 \\
&+ 2(C_{22}^{(4)}-C_{23}^{(4)})\hat{s} - 2C_0^{(4)}m_{d^I}^2\Big] + 4C_{24}^{(3)}F^V\Big\}
\end{aligned}
$$

The form factors of the amplitude part from quartic diagram are written as

$$
f_1^q = \frac{ig_s^2}{32\pi^2}F^V\Big[(-C_0^{(7)}-C_{11}^{(7)})m_c + C_{12}^{(7)}m_t\Big]
$$

References

[1] S.L.Glashow and S. Weinberg,Phys.Rev. D15,1958(1977).

[2] H.E. Haber and G.L. Kane, Phys. Rep. 117(1985)75.

[3] J.F. Gunion and H.E. Haber, Nucl. Phys. B272(1986)1.

[4] S.L. Glashow, Nucl. Phys. 22(1961)579; S. Weinberg, Phys. Rev. Lett. 1(1967)1264; A. Salam, Proc. 8th Nobel Symposium Stockholm 1968, ed. N. Svartholm(Almquist and Wiksells, Stockholm 1968) p.367; H.D. Politzer, Phys. Rep. 14(1974)129.

[5] P.W. Higgs, Phys. Lett 12(1964)132, Phys. Rev. Lett. 13 (1964)508; Phys.Rev. 145(1966)1156; F. Englert and R.Brout, Phys. Rev. Lett. 13(1964)321; G.S. Guralnik, C.R.Hagen and T.W.B. Kibble, Phys. Rev. Lett. 13(1964)585; T.W.B. Kibble, Phys. Rev. 155(1967)1554.

[6] "Proceeding of the Workshop on Physics and Experiments with Linear e^+e^- Colliders", eds. A.Miyamoto and Y.Fujii, World Scientific, Singapore, 1996.

[7] T. Han and J. Hewett, Phys.Rev. D60 (1999) 074015, hep-ph/9811237; U. Mahanta and A. Ghosal, Phys. Rev. **D57** (1998) 1735; Y. Koide, hep-ph/9701261; T. Han, M. Hosch, K. Whisnant, Bing-Lin Young, X. Zhang, Phys. Rev. D58 (1998) 073008.

[8] C.-H. Chang, X.-Q. Li, J.-X. Wang, and M.-Z. Yang, Phys. Lett. **B313** (1993) 389.

[9] David Atwood et al. Phys. Rev. **D53**, 1199(1996).

[10] Wei-Shu Hou and Guey-Lin Lin, Phys. Lett. **B379**, 261(1996).

[11] Y. Jiang, M.L. Zhou, W.G. Ma, L. Han, H. Zhou and M. Han, Phys.Rev.D57(1998).

[12] Z.H. Yu, H.Pietschmann,W.G. Ma, L.Han and Y. Jiang, Euro. Phys. C16 (2000) 695; Z.H. Yu, H.Pietschmann,W.G. Ma, L.Han and Y. Jiang, Euro. Phys. C16 (2000) 541.

[13] E. Malkawi and T. Tait, Phys. Rev. **D 54**, (1996) 5758.

[14] G. Eilam, J.L. Hewett and A. Soni, Phys. Rev. **D 44**, 1473 (1991).

[15] B. Grzadkowski, J.F. Gunion and P. Krawczyk, Phys. Lett. **B 268**, 106 (1991); M. Luke and M.J. Savage, Phys. Lett. **B 307**, 387 (1993); G. Couture, C. Hamzaoui and H. König, Phys. Rev. **D 52**, 1713 (1995); Jorge L. Lopez, D.V. Nanopoulos and Raghavan Rangarajan, Phys. Rev. **D 56**, 3100 (1997); T. P. Cheng and M. Sher, Phys. Rev. **D 48**, 3484 (1987); W.S. Hou, Phys. Lett. **B 296**, 179 (1992); L.J. Hall and S. Weinberg, Phys. Rev. **D 48**, 979 (1993); D. Atwood, L. Reina and A. Soni, Phys. Rev. **D 53**, 1199 (1996); Jin Min Yang, Bing-Lin Young, and X. Zhang, Phys.Rev. D58 (1998) 055001,hep-ph/9705341.

[16] Chong Sheng Li, Xinmin Zhang, Shou Hua Zhu, Phys.Rev. D60 (1999) 077702.

[17] Z.X. Chang, L. Han, Y. Jiang, W.G. Ma, H. Zhou and M.L. Zhou, Phys. Rev. D62(2000) 034012.

[18] S.Dimopoulos,G.F.Giudice and N.Tetradis, Nucl.Phys.B454(1995)59

[19] G.Farrar and P.Fayet,Phys. Lett. B76(1978)575.

[20] R. Barbieri et.al, hep-ph/9810232; B. Allanach et. al, hep-ph/9906224.

[21] B.C. Allanach,A. Dedes and H.K. Dreiner Phys.Rev. D60 (1999) 075014,hep-ph/9906209.

[22] L. Ibanez and G. G. Ross, Phys. Lett. B260 291 (1991), Nucl. Phys. B368 3 (1992);J. Ellis, S. Lola and G. G. Ross, Nucl. Phys. B526 115 (1998).

[23] L.H. Wan, W.G. Ma, Y. Jiang and L. Han, J. Phys.**G27** (2001)203.

[24] M. Gell-Mann, Phys. Rev. 125,1067(1962).

[25] Y. Jiang, W.G. Ma, L. Han, Z.H. Yu and H. Pietschmann, Phys. Rev. **D62** (2000)035006.

[26] A.D. Martin, W.J. Stirling and R.G. Roberts, Phys. Lett. B354, 155(1995).

[27] Particle Data Group, Euro.Phys. C15(2000)23,26

[28] M. Drees and S.P. Martin,hep-ph/9504324

[29] V. Barger, M. S. Berger and P. Ohmann, Phys. Rev. **D47**, 1093(1993), **D47**, 2038(1993); V. Barger, M. S. Berger, P. Ohmann and R. J. N. Phillips, Phys. Lett. **B314**, 351(1993); V. Barger, M. S. berger and P. Ohmann, Phys. Rev. **D49**, 4908(1994).

[30] Kniehl B. A., Phys. Rep. 240(1994)211 and references therein.

[31] G. Passarino and M. Veltman, Nucl. Phys. **B160**,(1979)151.

Figure Captions

Fig.1 The Feynman diagrams of the subproecesses $d\bar{d} \to t\bar{c} + \bar{t}c$ and $gg \to t\bar{c} + \bar{t}c$.

Fig.2 The subprocess cross sections as a function of $\sqrt{\hat{s}}$. The upper is of $d\bar{d} \to t\bar{c} + \bar{t}c$ and the lower is of $gg \to t\bar{c} + \bar{t}c$.

Fig.3 The folded cross sections as a function of $\tan\beta$ at LHC in the mSUGRA scenario.

Fig.4 The folded cross sections as a function of m_0 at LHC in the mSUGRA scenario.

Fig.5 The folded cross sections as a function of $\lambda'_{331} * \lambda'_{321}$ at LHC.

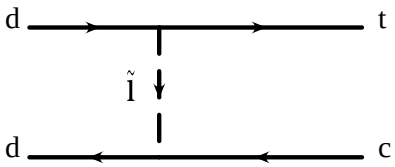

Fig.1a

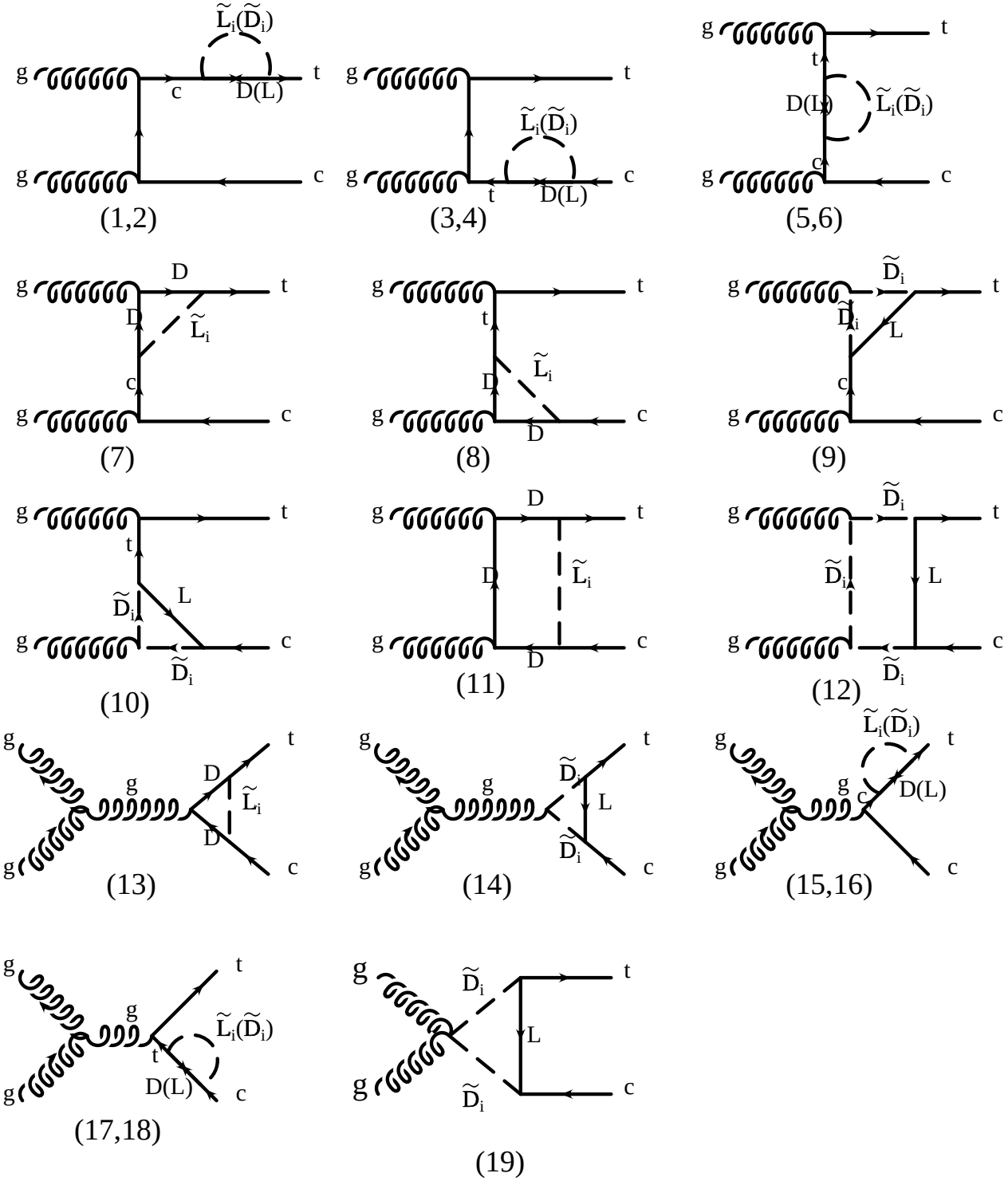

Fig.1b

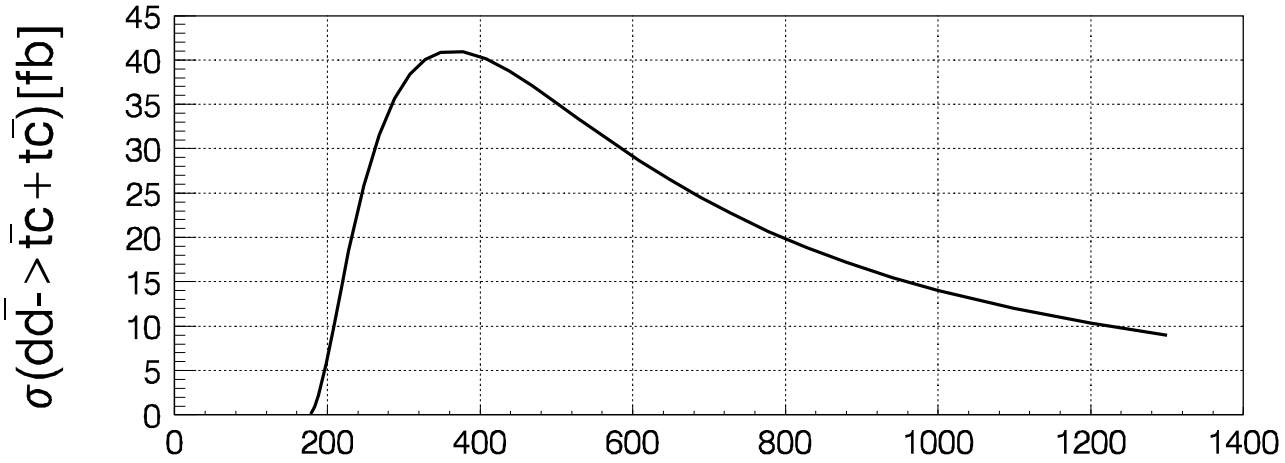
$\sigma(d\bar{d}->\bar{t}c+t\bar{c})[fb]$
45
40
35
30
25
20
15
10
5
0
0
200
400
600
800
1000
1200
1400

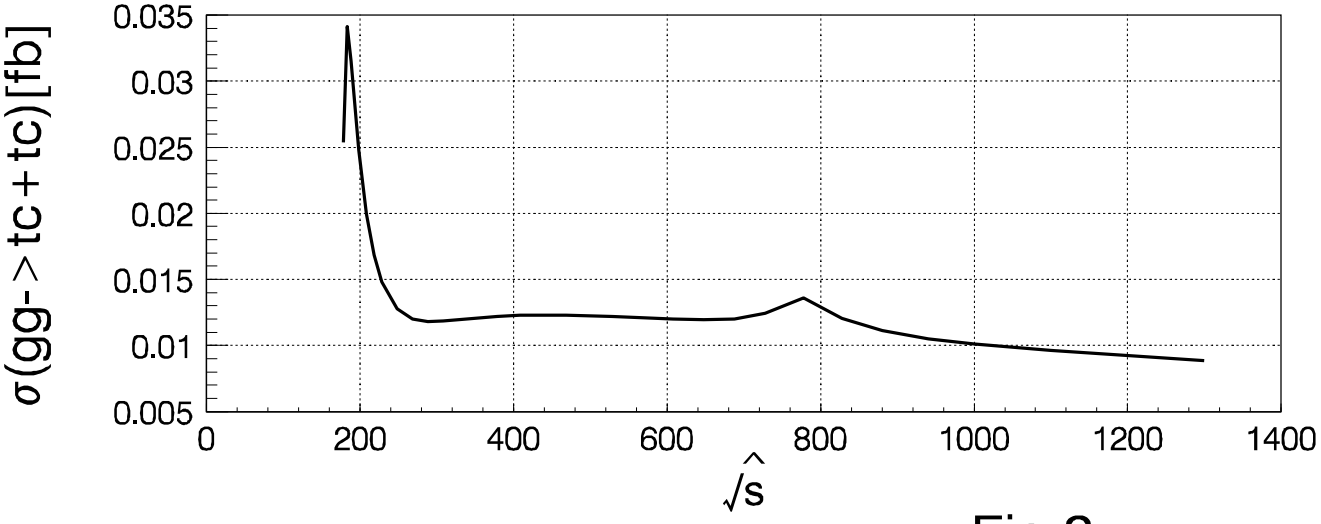
$\sigma(gg->\bar{t}c+t\bar{c})[fb]$
0.035
0.03
0.025
0.02
0.015
0.01
0.005
0
200
400
600
800
1000
1200
1400
$\sqrt{\hat{s}}$

Fig.2

Fig.3

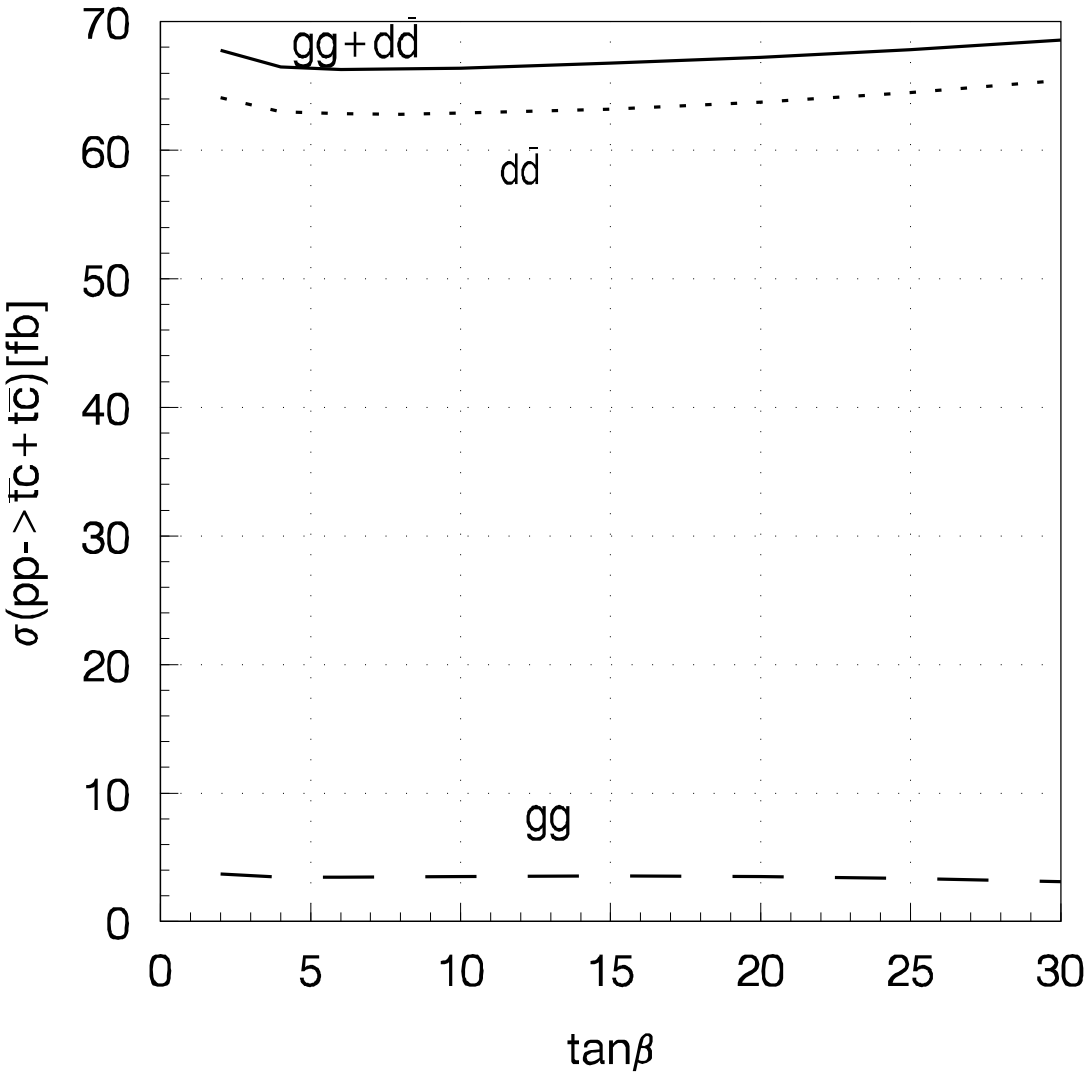

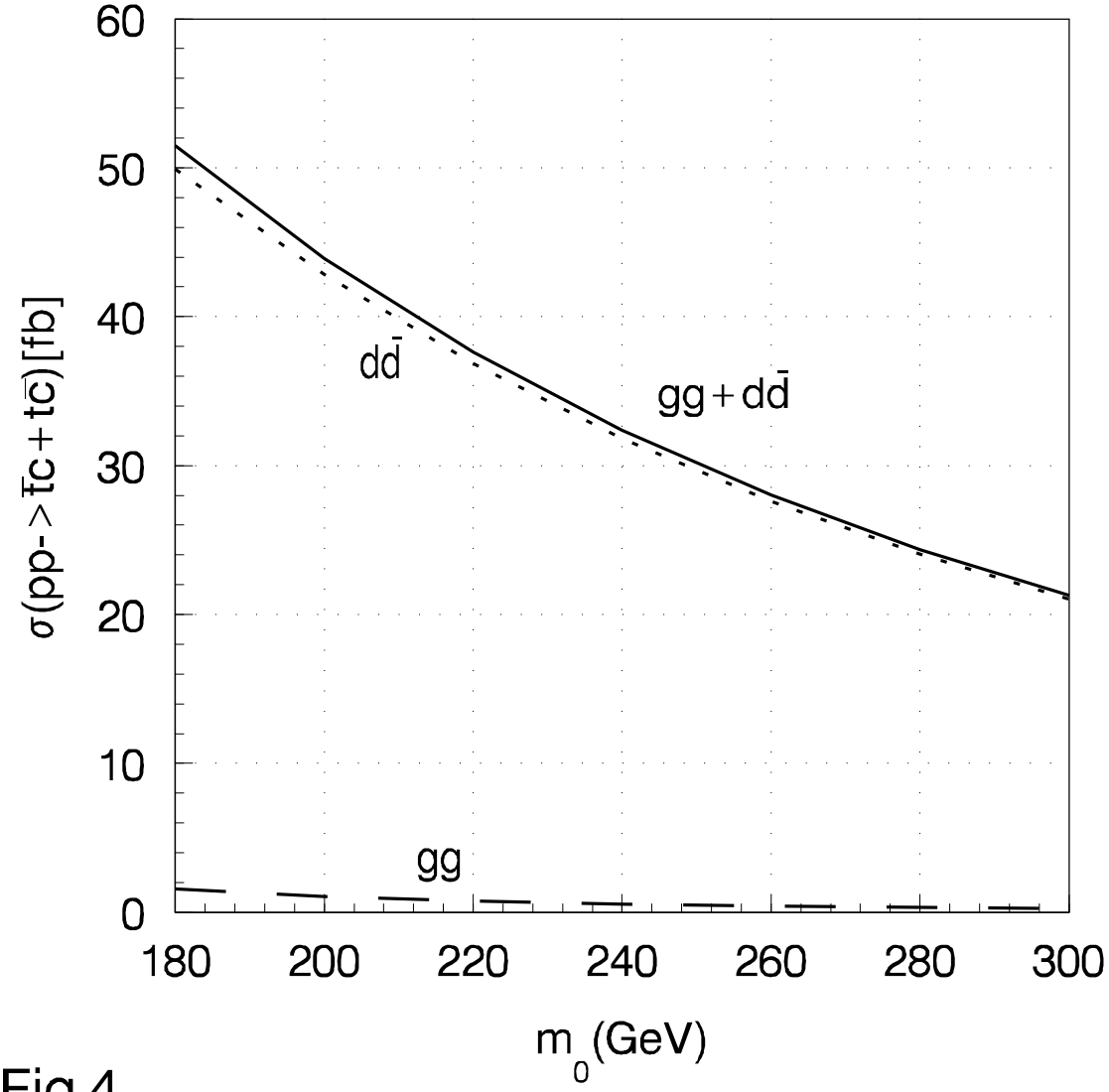
60
50
40
30
20
10
0
180
200
220
240
260
280
300
σ(pp->tc̄+t̄c)[fb]
m0(GeV)
dd̄
gg+dd̄
gg

Fig.4

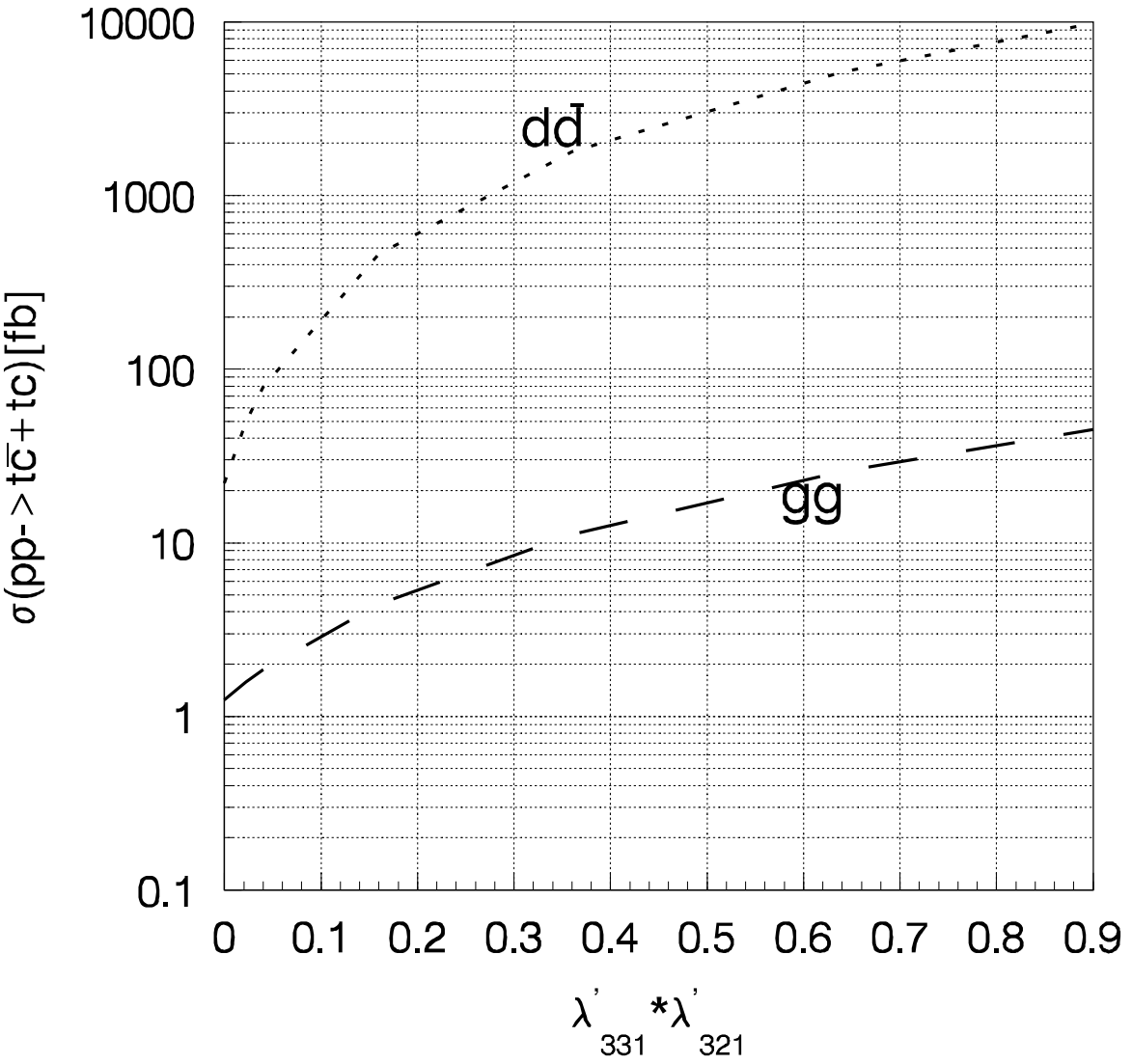
10000
1000
100
10
1
0.1
0
0.1
0.2
0.3
0.4
0.5
0.6
0.7
0.8
0.9
dd
gg
σ(pp->tc̄+t̄c)[fb]
λ'331*λ'321

Fig.5